INTERNATIONAL JOURNAL OF
NUMERICAL ANALYSIS AND MODELING
Volume 15, Number 1-2, Pages 170–192



# A FRACTIONAL STOKES EQUATION AND ITS SPECTRAL APPROXIMATION

SHIMIN LIN, MEJDI AZAÏEZ, AND CHUANJU XU†

**Abstract.** In this paper, we study the well-posedness of a fractional Stokes equation and its numerical solution. We first establish the well-posedness of the weak problem by suitably define the fractional Laplacian operator and associated functional spaces. The existence and uniqueness of the weak solution is proved by using the classical saddle-point theory. Then, based on the proposed variational framework, we construct an efficient spectral method for numerical approximations of the weak solution. The main contribution of this work are threefold: 1) a theoretical framework for the variational solutions of the fractional Stokes equation; 2) an efficient spectral method for solving the weak problem, together with a detailed numerical analysis providing useful error estimates for the approximative solution; 3) a fast implementation technique for the proposed method and investigation of the discrete system. Finally, some numerical experiments are carried out to confirm the theoretical results.

**Key words.** Fractional derivative, Stokes equations, well-posedness, spectral method.

## 1. Introduction

Fractional partial differential equations(FPDEs) are generalizations of the integer-order models, based on fractional calculus. As a useful tool in modelling the phenomenon related to nonlocality and memory effect, the FPDEs have been attracting increasing attention in recent years. They are now finding many applications in a broad range of fields such as control theory, biology, electrochemical processes, viscoelastic materials, polymer, finance, and etc; see, e.g.,[2, 3, 4, 5, 6, 16, 19, 21, 22, 31, 32, 33] and the references therein. In particular, fractional diffusion equations have been frequently used to describe the so-called anomalous diffusion phenomenon; see, e.g., [12, 15, 17, 35, 37, 38].

In this paper, we will consider sub-diffusion problems of the incompressible flows. This problem is related to the Navier-Stokes equation with sub-dissipation, which has been the subject of many research studies in the community of PDE theory. For example, Katz and Pavlović [20] considered the equations $\frac{\partial u}{\partial t} + (-\Delta)^\alpha u + u \cdot \nabla u + \nabla p = 0$, $\nabla \cdot u = 0$ with the initial condition $u(0, x) = u_0(x) \in C_c^\infty(\mathbb{R}^3)$, and proved that for this equation the Hausdorff dimension of the singular set at time of first blow up is at most $5 - 4\alpha$ and the solution has global regularity in the critical and subcritical hyper-dissipation regimes $\alpha \geq 5/4$. Tao [40] considered the global Cauchy problem for the same Navier-Stokes equations in $\mathbb{R}^d, d \geq 3$, and improved the above-mentioned result in the hyper-dissipation regimes under a slightly weaker condition. Yu & Zhai [43] investigated the well-posedness of the fractional Navier-Stokes equations in some supercritical Besov spaces and largest critical spaces. Xiao et al. [41] proved a general global well-posedness result for the fractional Navier-Stokes equations in some critical Fourier-Besov spaces.

On the other side, a considerable body of literature has been devoted to studying numerical methods for the FPDEs, it is impossible to give even a very brief

Received by the editors May 24, 2017 and, in revised form, October 04, 2017.
2000 *Mathematics Subject Classification.* 26A33, 35Q30, 49K40, 76M22.
†Corresponding author.

review here. Nevertheless, we refer to [26] for a review on the recent progress of high order numerical methods, particularly spectral methods, for the fractional differential equations. The main focus of the current paper is to set up a functional framework for the fractional Stokes equation in bounded domains, and propose a spectral method for its numerical solutions. As it has been well known for the traditional Stokes equation, a suitable variational formulation is essential for spectral methods to be efficient. The suitable weak form relies on the choice of the space pair for the velocity and pressure. The main contribution of this paper includes: first, we introduce the velocity and pressure spaces such that the associated saddle point problem is well-posed; secondly, we construct an efficient spectral method for numerical approximations of the weak solution. Based on the weak formulation and the polynomial approximation results in the related Sobolev spaces, we are able to derive some error estimates. Finally we present an implementation technique of the algorithm, and some numerical results to confirm the theoretical statements.

The rest of the paper is organized as follows: In the next section we recall some notations of fractional calculus and list some lemmas which will be used in the following sections. In Section 3 the fractional Stokes problem is studied and the well-posedness result is established. Then we propose and analyze in Section 4 a stable spectral method based on weak formulation, and derive the error estimates for the numerical solution. In Section 5, we give some implementation details and present the numerical results to support the theoretical statements. In Section 6, we present an extension to the fractional Navier-Stokes equations. Some concluding remarks are given in the final section.

## 2. Preliminaries

In this section, we present some notations and basic properties of fractional calculus [1, 13, 34, 24, 36]. which will be used throughout the paper. Let $\mathbb{N}$ and $\mathbb{R}$ be the set of positive integers and real numbers respectively, and set $\mathbb{N}_0 := \{0\} \cup \mathbb{N}$. Let $c$ be a generic positive constant independent of any functions and of any discretization parameters. We use the expression $A \lesssim B$ (respectively, $A \gtrsim B$) to mean that $A \le cB$ (respectively, $A \ge cB$), and use the expression $A \cong B$ to mean that $A \lesssim B \lesssim A$. In all that follows, without lose of generality, we set $\Lambda = (-1, 1)$ and $\Omega_d = \Lambda^d$. The generic points of $\Omega_d$ is denoted by $\boldsymbol{x} = (x_1, \cdots, x_d)$. In some specific occurrences, we may use $(x, y)$ to represent the generic points of $\Omega_d$ when $d = 2$ ($(x, y, z)$ when $d = 3$), and use $\Omega$ instead of $\Omega_d$ to represent the domain for simplification.

**Definition 2.1** (RL fractional integral)**.** *Let $f(x)$ be Riemann integrable on $(a, b)$, $-\infty < a < b < \infty$. The left-sided and right-sided Riemann-Liouville fractional integral of order $s > 0$ are defined by*

$$ {}_aI_x^s f(x) := \frac{1}{\Gamma(s)} \int_a^x (x-t)^{s-1} f(t)\, dt, \qquad {}_xI_b^s f(x) := \frac{1}{\Gamma(s)} \int_x^b (t-x)^{s-1} f(t)\, dt $$

*respectively, where $\Gamma(\cdot)$ is the Gamma function.*

**Definition 2.2** (RL fractional derivative)**.** *For a given $f(x)$, the Riemann-Liouville fractional derivatives ${}_aD_x^s f$ and ${}_xD_b^s f$ of order $s > 0$ are defined by*

$$ {}_aD_x^s f(x) := \frac{d^n}{dx^n} {}_aI_x^{n-s} f(x) = \frac{1}{\Gamma(n-s)} \frac{d^n}{dx^n} \int_a^x (x-t)^{n-s-1} f(t)\, dt, \;\; n = \lceil s \rceil, $$

*and*

$${}_xD_b^s f(x) := (-1)^n \frac{d^n}{dx^n} {}_xI_b^{n-s} f(x) = \frac{(-1)^n}{\Gamma(n-s)} \frac{d^n}{dx^n} \int_x^b (t-x)^{n-s-1} f(t)\, dt, \;\; n = \lceil s \rceil$$

*respectively, where* $\lceil s \rceil$ *means the smallest integer such that* $\lceil s \rceil \geq s$.

**Definition 2.3** (Caputo fractional derivative)**.** *For a given* $f(x)$*, the Caputo fractional derivatives* ${}_a^CD_x^s f$ *and* ${}_x^CD_b^s f$ *of order* $s > 0$ *are defined by*

$${}_a^CD_x^s f(x) := {}_aI_x^{n-s} f^{(n)}(x) = \frac{1}{\Gamma(n-s)} \int_a^x (x-t)^{n-s-1} f^{(n)}(t)\, dt, \;\; n = \lceil s \rceil,$$

*and*

$${}_x^CD_b^s f(x) := (-1)^n {}_xI_b^{n-s} f^n(x) = \frac{(-1)^n}{\Gamma(n-s)} \int_x^b (t-x)^{n-s-1} f^{(n)}(t)\, dt, \;\; n = \lceil s \rceil$$

*respectively.*

The relation between Riemann-Liouville and Caputo derivative is given as follows.

**Lemma 2.1.** [14] *Let* $n \in \mathbb{N}, n-1 \leq s < n$*, then we have*

$${}_aD_x^s f(x) = {}_a^CD_x^s f(x) + \sum_{j=0}^{n-1} \frac{f^{(j)}(a)}{\Gamma(1+j-s)} (x-a)^{j-s};$$

$${}_xD_b^s f(x) = {}_x^CD_b^s f(x) + \sum_{j=0}^{n-1} \frac{(-1)^j f^{(j)}(b)}{\Gamma(1+j-s)} (b-x)^{j-s}.$$

Next we list a number of formulas related to the fractional integrals and derivatives of the Jacobi polynomials. These formulas are useful in implementing the proposed numerical method. We recall that the Jacobi polynomials, denoted by $J_n^{s,\sigma}(x)$ for $s, \sigma > -1$, are orthogonal with respect to the Jacobi weight function $\omega^{s,\sigma}(x) := (1-x)^s(1+x)^\sigma$ over $\Lambda$, namely,

$$\int_{-1}^1 J_n^{s,\sigma}(x) J_m^{s,\sigma}(x) \omega^{s,\sigma}(x)\, dx = \gamma_n^{s,\sigma} \delta_{mn},$$

where $\delta_{mn}$ is the Kronecker-delta symbol and

$$\gamma_n^{s,\sigma} = \frac{2^{s+\sigma+1}\Gamma(n+s+1)\Gamma(n+\sigma+1)}{(2n+s+\sigma+1)n!\Gamma(n+s+\sigma+1)}.$$

The Jacobi polynomials for parameters $s \leq -1$ and/or $\sigma \leq -1$ are defined as in Szegö [39]. Then we have the following two lemmas.

**Lemma 2.2.** *(*[44] *Lemma 3.2 and* [13] *Lemma 2.4) Let* $\rho > 0, n \in \mathbb{N}_0$*, and* $x \in \Lambda$*.*

- *For* $s \in \mathbb{R}$ *and* $\sigma > -1$*,*

$$(1) \qquad {}_{-1}I_x^\rho \{(1+x)^\sigma J_n^{s,\sigma}(x)\} = \frac{\Gamma(n+\sigma+1)}{\Gamma(n+\sigma+\rho+1)} (1+x)^{\sigma+\rho} J_n^{s-\rho,\sigma+\rho}(x).$$

- *For* $s > -1$ *and* $\sigma \in \mathbb{R}$*,*

$$(2) \qquad {}_xI_1^\rho \{(1-x)^s J_n^{s,\sigma}(x)\} = \frac{\Gamma(n+s+1)}{\Gamma(n+s+\rho+1)} (1-x)^{s+\rho} J_n^{s+\rho,\sigma-\rho}(x).$$

**Lemma 2.3.** *(*[13] *Lemma 2.5) Let* $\rho > 0, n \in \mathbb{N}_0$*, and* $x \in \Lambda$*.*

- *For* $s \in \mathbb{R}$ *and* $\sigma > -1$,

$$ {}_{-1}D_x^{\rho}\{(1+x)^{\sigma+\rho} J_n^{s-\rho,\sigma+\rho}(x)\} = \frac{\Gamma(n+\sigma+\rho+1)}{\Gamma(n+\sigma+1)}(1+x)^{\sigma} J_n^{s,\sigma}(x). \tag{3} $$

- *For* $s > -1$ *and* $\sigma \in \mathbb{R}$,

$$ {}_{x}D_1^{\rho}\{(1-x)^{s+\rho} J_n^{s+\rho,\sigma-\rho}(x)\} = \frac{\Gamma(n+s+\rho+1)}{\Gamma(n+s+1)}(1-x)^{s} J_n^{s,\sigma}(x). \tag{4} $$

We now introduce some Sobolev spaces, which will be used to define the weak problem for the fractional Stokes equation. $L^2(\Omega_d)$ is defined as the space of functions which are square measurable. The associated inner product and norm are denoted by

$$ (u,v)_{\Omega_d} := \int_{\Omega_d} uv\, d\boldsymbol{x}, \quad \|u\|_{L^2(\Omega_d)} := (u,u)_{\Omega_d}^{\frac{1}{2}}, \quad \forall u,v \in L^2(\Omega_d). $$

For a nonnegative real number $s$, $H^s(\Omega_d)$ and $H_0^s(\Omega_d)$ denote the usual Sobolev space with norm $\|\cdot\|_{s,\Omega_d}$ and semi-norm $|\cdot|_{s,\Omega_d}$. Let $E$ be a separable Hilbert space for norm $\|\cdot\|_E$. For any positive real number $s$, we consider space

$$ H^s(\Lambda; E) = \{\|v(x,\cdot)\|_E \in H^s(\Lambda)\}, $$

equipped with the norm

$$ \|v\|_{H^s(\Lambda;E)} = \|\|v(x,\cdot)\|_E\|_{s,\Lambda}. $$

With each function $v$ in $L^2(\Omega_d)$, we associate the $d$-functions $v_j$ defined by

$$ v_j(x_j)(x_1,\cdots,x_{j-1},x_{j+1},\cdots,x_d) = v(x_1,\cdots,x_d), \quad 1 \le j \le d. $$

Then for any $j$, $1 \le j \le d$, and for any nonnegative real numbers $s,\sigma$, we define the space

$$ H^s(\Lambda_j; H^{\sigma}(\Omega_{d-1})) = \{v \in L^2(\Omega_d); v_j \in H^s(\Lambda_j; H^{\sigma}(\Omega_{d-1}))\}, $$

where, although $\Lambda_j$ is always equal to $\Lambda$ for all $j = 1,\ldots,d$, the subscript $j$ is used to mean the domain for the $j^{th}$ variable.

The following properties of the tensorized spaces can be found in [9]:

- For any $j$, $1 \le j \le d$,

$$ L^2(\Omega_d) = L^2(\Lambda_j; L^2(\Omega_{d-1})). \tag{5} $$

- For any nonnegative real number $s$ and $\sigma$, $\sigma \le s$, the following embedding holds:

$$ H^s(\Omega_d) \subset H^{\sigma}(\Lambda_j; H^{s-\sigma}(\Omega_{d-1})). \tag{6} $$

- For any nonnegative real number $s$, it holds

$$ H^s(\Omega_d) = \bigcap_{j=1}^{d} H^s(\Lambda_j; L^2(\Omega_{d-1})). \tag{7} $$

**Lemma 2.4.** [24] *For* $0 < s < 1, s \ne \frac{1}{2}$, *if* $w,v \in H_0^s(\Lambda)$, *then*

$$ ({}_{-1}D_x^s\,{}_{-1}D_x^s w, v)_{\Lambda} = ({}_{-1}D_x^s w, {}_xD_1^s v)_{\Lambda}, \quad ({}_xD_1^s\,{}_xD_1^s w, v)_{\Lambda} = ({}_xD_1^s w, {}_{-1}D_x^s v)_{\Lambda}, $$
$$ ({}_xD_1^s\,{}_{-1}D_x^s w, v)_{\Lambda} = ({}_{-1}D_x^s w, {}_{-1}D_x^s v)_{\Lambda}, \quad ({}_{-1}D_x^s\,{}_xD_1^s w, v)_{\Lambda} = ({}_xD_1^s w, {}_xD_1^s.v)_{\Lambda}. $$

**Lemma 2.5.** [24] *Let* $s > 0, s \ne n - \frac{1}{2}, n \in \mathbb{N}$, *for* $\forall v \in H_0^s(\Lambda)$, *we have*

$$ ({}_{-1}D_x^s v, {}_xD_1^s v)_{\Lambda} \cong \cos(\pi s)\|{}_{-1}D_x^s v\|_{L^2(\Lambda)}^2 \cong \cos(\pi s)\|{}_xD_1^s v\|_{L^2(\Lambda)}^2 \cong \cos(\pi s)\|v\|_{s,\Lambda}^2. $$

In what follows, for the sake of simplification, the left-sided and right-sided derivatives will be denoted by $D^s_x, {}_xD^s$, and similar simplifications will be used for other notations. The domain symbol in the subscript of norms may be dropped if no confusion would arise.

## 3. Fractional Stokes equation

We consider the fractional Stokes equations as follows: for $\boldsymbol{f}(\boldsymbol{x})$ given, find the velocity and pressure $(\boldsymbol{u}, p)$, such that

$$-\Delta^\alpha \boldsymbol{u} + \nabla p = \boldsymbol{f}, \quad \text{in } \Omega_d, \tag{8}$$

$$\nabla \cdot \boldsymbol{u} = 0, \quad \text{in } \Omega_d, \tag{9}$$

$$\boldsymbol{u} = 0, \quad \text{on } \partial\Omega_d, \tag{10}$$

where $\frac{1}{2} < \alpha \leq 1, d = 2, 3$. At this first step of research, we consider a symmetric definition for the fractional Laplacian operator; see [38]:

$$-\Delta^\alpha := -\frac{1}{4}\sum_{j=1}^{d}\left(D^\alpha_{x_j} - {}_{x_j}D^\alpha\right)\left({}^C D^\alpha_{x_j} - {}^C_{x_j}D^\alpha\right). \tag{11}$$

**Remark 3.1.** *There are some other definitions of fractional Laplacian operator, such as the Fourier transform definition, the Riesz fractional derivative etc. Under some suitable assumptions, some of them are equivalent. For example, in one dimensional domain* $\Lambda$*, under the homogeneous boundary condition, the Fourier transform definition is equivalent to definition*[42]*:*

$$-\Delta^\alpha := -(D^{2\alpha}_x +_x D^{2\alpha}) \tag{12}$$

*Obviously our definition* (11) *is a more general definition than* (12).

To define weak problem of the above Stokes equation, we introduce the following space:

$$X := \{\boldsymbol{v} \in H^\alpha_0(\Omega_d)^d;\ \nabla \cdot \boldsymbol{v} \in L^2(\Omega_d)\},$$

endowed with the norm

$$\|\boldsymbol{v}\|_X := \left(\|\boldsymbol{v}\|^2_\alpha + \|\nabla \cdot \boldsymbol{v}\|^2_0\right)^{\frac{1}{2}}. \tag{13}$$

Obviously, $\|\boldsymbol{v}\|_X \lesssim \|\boldsymbol{v}\|_1$ for all $\boldsymbol{v} \in H^1(\Omega_d)^d$. For the pressure, we define the space

$$M := \left\{q \in L^2(\Omega_d) : \int_{\Omega_d} q(\boldsymbol{x})d\boldsymbol{x} = 0\right\}.$$

Inspired by Lemma 2.1 and Lemma 2.4, we consider the weak formulation of (8)-(10) as follows: given $\boldsymbol{f} \in X'$, the dual space of $X$, find $(\boldsymbol{u}, p)$ in $X \times M$, such that

$$a(\boldsymbol{u}, \boldsymbol{v}) + b(\boldsymbol{v}, p) = \langle \boldsymbol{f}, \boldsymbol{v}\rangle, \quad \forall \boldsymbol{v} \in X, \tag{14}$$

$$b(\boldsymbol{u}, q) = 0, \quad \forall q \in M, \tag{15}$$

where $\langle\cdot,\cdot\rangle$ is the duality pairing. The bilinear forms $a(\cdot,\cdot)$ and $b(\cdot,\cdot)$ are defined respectively by: for $\boldsymbol{u} = (u^1, \cdots, u^d), \boldsymbol{v} = (v^1, \cdots, v^d)$,

$$\begin{aligned} a(\boldsymbol{u}, \boldsymbol{v}) : &= -\frac{1}{4}\sum_{i=1}^{d}\sum_{j=1}^{d}\Big[\left(D^\alpha_{x_j}u^i, {}_{x_j}D^\alpha v^i\right) + \left({}_{x_j}D^\alpha u^i, D^\alpha_{x_j}v^i\right) \\ &\qquad - \left(D^\alpha_{x_j}u^i, D^\alpha_{x_j}v^i\right) - \left({}_{x_j}D^\alpha u^i, {}_{x_j}D^\alpha v^i\right)\Big], \\ b(\boldsymbol{v}, q) : &= -(\nabla \cdot \boldsymbol{v}, q). \end{aligned}$$

Obviously, the definition (11) for the fractional Laplacian makes the bilinear form $a(\cdot,\cdot)$ symmetric.

**Remark 3.2.** *We have to be very cautious with formulation of the FPDEs. The use of the mixed fractional derivatives is advantageous than a single derivative, especially when dealing with non homogeneous boundary conditions. For example, considering the equation using RL derivatives with non homogeneous boundary condition as follows:*

$$\begin{cases} -{}_{-1}D_x^{1.6}u = f, & x \in \Lambda, \\ u(-1) = u(1) = 1. \end{cases} \tag{16}$$

*For a given $f(x) = 1$, if the solution $u(x)$ of equation* (16) *belongs to $H^{0.8}(\Lambda) \subset C(\bar{\Lambda})$, then it can be verified that the solution can be written in following form:*

$$u(x) = -{}_{-1}I_x^{1.6}f(x) + c_1(x+1)^{0.6} + c_2(x+1)^{-0.4} \tag{17}$$

*$c_1, c_2$ are two constants determined by boundary condition. We find that only $c_2 = 0$ can lead to $u(x) \in H^{0.8}(\Lambda)$. However, $u(-1) = 0 \neq 1$ when $c_2 = 0$. i.e. the solution in form* (17) *would never satisfy the boundary condition. In contrary, the following problem*

$$\begin{cases} -{}_{-1}D_x^{0.8}\,{}_{-1}^{C}D_x^{0.8}u = 1, & x \in \Lambda, \\ u(-1) = u(1) = 1 \end{cases}$$

*admits a solution $u = ((x+1)^{0.6}(1-x))/\Gamma(2.6) + 1 \in H^{0.8}(\Lambda)$.*

In order to establish the well-posedness of (14)-(15), we define the kernel space

$$K := \{\boldsymbol{v} \in X : b(\boldsymbol{v}, q) = 0, \ \forall q \in M\}. \tag{18}$$

**Theorem 3.1.** *The weak problem (14)-(15) is well-posed.*

*Proof.* First according to the definitions of the bilinear forms $a(\cdot,\cdot)$ and $b(\cdot,\cdot)$ and the spaces $X$ and $M$, it is readily seen that $a(\cdot,\cdot)$ and $b(\cdot,\cdot)$ are both continuous in the spaces in which they are defined. Furthermore, using Lemma 2.5 and property (7), for $\forall \boldsymbol{v} \in K$, there exists a positive constant $\delta$ such that

$$\begin{aligned} a(\boldsymbol{v},\boldsymbol{v}) = &-\frac{1}{4}\sum_{i=1}^{d}\sum_{j=1}^{d}\Big[\Big(D_{x_j}^{\alpha}v^i,\, {}_{x_j}D^{\alpha}v^i\Big) + \Big({}_{x_j}D^{\alpha}v^i, D_{x_j}^{\alpha}v^i\Big) \\ &\qquad - \Big(D_{x_j}^{\alpha}v^i, D_{x_j}^{\alpha}v^i\Big) - \big({}_{x_j}D^{\alpha}v^i,\, {}_{x_j}D^{\alpha}v^i\big)\Big] \\ \gtrsim &\sum_{i=1}^{d}\sum_{j=1}^{d}\Big[\|D_{x_j}^{\alpha}v^i\|^2_{L^2(\Omega_d)} + \big\|{}_{x_j}D^{\alpha}v^i\big\|^2_{L^2(\Omega_d)}\Big] \\ \gtrsim &\sum_{i=1}^{d}\sum_{j=1}^{d}\|v^i\|^2_{H^{\alpha}(\Lambda_j;L^2(\Omega_{d-1}))} \gtrsim \sum_{i=1}^{d}\|v^i\|^2_{\alpha} \geq \delta\|\boldsymbol{v}\|^2_X. \end{aligned}$$

That is, $a(\cdot,\cdot)$ is coercive. Thus there exists a unique solution $\boldsymbol{u}$ to (14)-(15). On the other side, it is well known [9, 18] that for any $q \in M$, there exists $\boldsymbol{w} \in H_0^1(\Omega_d)^d \subset X$, such that

$$-\nabla\cdot\boldsymbol{w} = q, \quad \|\boldsymbol{w}\|_1 \lesssim \|q\|_0.$$

Thus we have

$$\sup_{\boldsymbol{v}\in X}\frac{b(\boldsymbol{v},q)}{\|\boldsymbol{v}\|_X} = \sup_{\boldsymbol{v}\in X}\frac{-(\nabla\cdot\boldsymbol{v},q)}{\|\boldsymbol{v}\|_X} \geq \frac{\|q\|_0^2}{\|\boldsymbol{w}\|_X} \geq \frac{\|q\|_0^2}{\|\boldsymbol{w}\|_1} \gtrsim \|q\|_0,$$

which means $b(\cdot,\cdot)$ satisfies the *Inf-Sup* condition. Finally, in virtue of the standard saddle point theory [11], the problem (14)-(15) admits a unique solution. □

## 4. A stable spectral method

This section is devoted to construct a spectral method for the weak problem (14)–(15), and carry out numerical analysis for the proposed method. To alleviate the presentation, we will restrict ourself to the case $d = 2$ in the construction of the method, however the error analysis will be carried out for both 2D and 3D cases.

For a fixed integer $N \geq 2$, $\mathbb{P}_N(\Omega)$ denotes the space of polynomials of degree $\leq N$ with respect to each space variable. We denote the Jacobi-Gauss-Lobatto nodes, i.e., the zeros of $(1-\xi^2)J_{N-1}^{s+1,\sigma+1}(\xi)$ on the interval $\Lambda$, by $(\xi_{N,i}^{s,\sigma})_{0\leq i\leq N}$, and corresponding weights by $(\omega_{N,i}^{s,\sigma})_{0\leq i\leq N}$. Denote the Jacobi-Gauss nodes, i.e., the zeros of $J_{N+1}^{s,\sigma}$, by $(\eta_{N,i}^{s,\sigma})_{0\leq i\leq N}$, and corresponding weights by $(\rho_{N,i}^{s,\sigma})_{0\leq i\leq N}$. Assume that $u$ and $v$ are continuous functions, we define the discrete scalar products:

$$
\begin{aligned}
(u,v)_{x,N} &:= \sum_{i=0}^{N}\int_\Lambda u(\xi_{N,i}^{0,0},y)v(\xi_{N,i}^{0,0},y)\omega_{N,i}^{0,0}\,dy,\\
(u,v)_{y,N} &:= \sum_{j=0}^{N}\int_\Lambda u(x,\xi_{N,j}^{0,0})v(x,\xi_{N,j}^{0,0})\omega_{N,j}^{0,0}\,dx,\\
(u,v)_{N} &:= \sum_{i,j=0}^{N} u(\xi_{N,i}^{0,0},\xi_{N,j}^{0,0})v(\xi_{N,i}^{0,0},\xi_{N,j}^{0,0})\omega_{N,i}^{0,0}\omega_{N,j}^{0,0},
\end{aligned}
$$

and their associated norms

$$
\|v\|_{x,N} = (v,v)_{x,N}^{\frac12},\quad \|v\|_{y,N} = (v,v)_{y,N}^{\frac12},\quad \|v\|_{N} = (v,v)_{N}^{\frac12}.
$$

The following equivalence is known (see e.g., [8]):

$$
\|v_N\|_{x,N} \cong \|v_N\|_{y,N} \cong \|v_N\|_N \cong \|v_N\|_0,\quad \forall v_N \in \mathbb{P}_N(\Lambda). \tag{19}
$$

We have to be careful in making choice of the discrete velocity and pressure space. As it has been well-known that the discrete pressure space has to be smaller than the velocity space for spectral approximation to the traditional Stokes equation. A common choice, suggested by Maday and Patera [30], is the so-called $\mathbb{P}_N \times \mathbb{P}_{N-2}$ method. Inspired by this fact, we are led to consider the same space pair for the fractional Stokes equation.

We set the discrete velocity space $X_N := \mathbb{P}_N(\Omega)^d \cap X$, and the pressure space $M_N := \mathbb{P}_{N-2}(\Omega) \cap M$.

Consider the spectral approximation to (14)–(15) as follows: find $(\boldsymbol{u}_N, p_N) \in X_N \times M_N$ such that

$$
\begin{aligned}
a_N(\boldsymbol{u}_N,\boldsymbol{v}_N) + b_N(\boldsymbol{v}_N,p_N) &= (\boldsymbol{f},\boldsymbol{v}_N)_N, \qquad \forall \boldsymbol{v}_N \in X_N, &(20)\\
b_N(\boldsymbol{u}_N,q_N) &= 0, \qquad \forall q_N \in M_N, &(21)
\end{aligned}
$$

where

$$
\begin{aligned}
(22)\qquad a_N(\boldsymbol{u}_N,\boldsymbol{v}_N) := -\frac{1}{4}\sum_{i=1}^{2}\Big[ & \big({}_xD^\alpha u_N^i, D_x^\alpha v_N^i\big)_{y,N} + \big(D_x^\alpha u_N^i,\ {}_xD^\alpha v_N^i\big)_{y,N} \\
& - \big(D_x^\alpha u_N^i, D_x^\alpha v_N^i\big)_{y,N} - \big({}_xD^\alpha u_N^i,\ {}_xD^\alpha v_N^i\big)_{y,N} \\
& + \big(D_y^\alpha u_N^i,\ {}_yD^\alpha v_N^i\big)_{x,N} + \big({}_yD^\alpha u_N^i, D_y^\alpha v_N^i\big)_{x,N} \\
& - \big(D_y^\alpha u_N^i, D_y^\alpha v_N^i\big)_{x,N} - \big({}_yD^\alpha u_N^i,\ {}_yD^\alpha v_N^i\big)_{x,N}\Big],
\end{aligned}
$$

$$(23)\qquad b_N(\boldsymbol{v}_N, q_N) := -(\nabla\cdot\boldsymbol{v}_N, q_N)_N,$$

with the convention $\boldsymbol{u} = (u_N^1, u_N^2)^T, \boldsymbol{v} = (v_N^1, v_N^2)^T$. These two bilinear forms in the 3D case can be defined in a similar way. We want to emphasize that in the above discretization, numerical quadratures are only used in the direction in which non fractional derivatives are applied. We know that the fractional derivative of a polynomial is no longer a polynomial, and naive applications of the numerical quadratures of Gauss type would result in a lose of accuracy. In our implementation, we will use an efficient way to evaluate the integrals.

Let

$$(24)\qquad K_N = \{\boldsymbol{v}_N \in X_N :\ b_N(\boldsymbol{v}_N, q_N) = 0,\ \forall q_N \in M_N\}.$$

We have the following theorem.

**Theorem 4.1.** *The spectral approximation problem (20)-(21) is well-posed.*

*Proof.* Similar to Theorem 3.1, the proof makes use of the saddle point theory. Once again, the continuities of the bilinear forms $a_N(\cdot,\cdot)$ and $b_N(\cdot,\cdot)$ are immediate. However, in the discrete case, $a_N(\cdot,\cdot)$ loses the uniform coercivity in $K_N \times K_N$ because the functions of $K_N$ are not necessarily divergence-free. Nevertheless, in virtue of (19) and the inverse inequality [7]

$$(25)\qquad |v_N|_1 \lesssim N^{2(1-\alpha)}|v_N|_\alpha,\quad \forall v_N \in \mathbb{P}_N(\Lambda),$$

we have

$$(26)\qquad a_N(\boldsymbol{v}_N,\boldsymbol{v}_N) \gtrsim \sum_{i=1}^{2}\|v_N^i\|_\alpha^2 \gtrsim \delta_N\|\boldsymbol{v}_N\|_X^2,$$

where $\delta_N = O(N^{4\alpha-4})$. It remains to prove the *Inf-Sup* condition of $b_N(\cdot,\cdot)$. It is known [10] that for $\forall q_N \in M_N$, there exists $\boldsymbol{w}_N \in X_N$ such that

$$(-\nabla\cdot\boldsymbol{w}_N, \varphi_N) = (q_N, \varphi_N),\quad \forall \varphi_N \in \mathbb{P}_{N-2}(\Omega),$$

and

$$\|\boldsymbol{w}_N\|_1 \lesssim N^{\frac{1}{2}}\|q_N\|_0.$$

Therefore we obtain

$$\sup_{\boldsymbol{v}_N\in X_N}\frac{-(\nabla\cdot\boldsymbol{v}_N, q_N)}{\|\boldsymbol{v}_N\|_X} \geq \frac{\|q_N\|_0^2}{\|\boldsymbol{w}_N\|_1} \gtrsim \beta_N\|q_N\|_0,$$

where $\beta_N = O(N^{-\frac{1}{2}})$. This completes the proof. □

Next we will derive an error estimate for the numerical solution. To this end, we first establish the following approximation result, which is an extension of some existing results in 1D and integer order cases.

**Lemma 4.1.** *Let $p$ and $\gamma$ be two real numbers such that $p \neq n + 1/2$, $n \in \mathbb{N}$, $0 \leq \gamma \leq p$, there exists an operator $\Pi_{p,N}^{\gamma,0}$ from $H^p(\Omega) \cap H_0^\gamma(\Omega)$ onto $\mathbb{P}_N(\Omega) \cap H_0^\gamma(\Omega)$, such that, for any $\varphi \in H^\sigma(\Omega) \cap H_0^\gamma(\Omega)$ with $\sigma \geq p$, we have*

$$\|\varphi - \Pi_{p,N}^{\gamma,0}\varphi\|_\nu \lesssim N^{\nu-\sigma}\|\varphi\|_\sigma, \;\; 0 \leq \nu \leq p. \tag{27}$$

*Proof.* The result in the case $d = 1$ has been proved in [28]. Here we want to demonstrate that it is also true in the case $d = 2$. Using Theorem 2.1 in [28], there exists an operator $\pi_N^{\gamma,0}$ from $H^p(\Lambda) \cap H_0^\gamma(\Lambda)$ onto $\mathbb{P}_N(\Lambda) \cap H_0^\gamma(\Lambda)$, such that, for any $\varphi \in H^\sigma(\Lambda) \cap H_0^\gamma(\Lambda), \sigma \geq p$,

$$\|\varphi - \pi_N^{\gamma,0}\varphi\|_{\nu,\Lambda} \lesssim N^{\nu-\sigma}\|\varphi\|_{\sigma,\Lambda}, \;\; 0 \leq \nu \leq p. \tag{28}$$

Now we define the operator $\Pi_{p,N}^{\gamma,0} : H^p(\Omega) \cap H_0^\gamma(\Omega) \to \mathbb{P}_N(\Omega) \cap H_0^\gamma(\Omega)$ by: $\forall \varphi \in H^p(\Omega) \cap H_0^\gamma(\Omega)$,

$$\Pi_{p,N}^{\gamma,0}\varphi = \pi_{N,y}^{\gamma,0}\pi_{N,x}^{\gamma,0}\varphi,$$

where $\pi_{N,i}^{\gamma,0}$ $(i = x, y)$ be the operator $\pi_N^{\gamma,0}$ acting in the $i$ direction. Then we have, $\forall \varphi \in H^\sigma(\Omega) \cap H_0^\gamma(\Omega), \sigma \geq p$,

$$\begin{aligned} \|\varphi - \Pi_{p,N}^{\gamma,0}\varphi\|_\nu =& \|\varphi - \pi_{N,y}^{\gamma,0}\pi_{N,x}^{\gamma,0}\varphi\|_\nu \\ \lesssim& \|\varphi - \pi_{N,y}^{\gamma,0}\pi_{N,x}^{\gamma,0}\varphi\|_{H^\nu(\Lambda;L^2(\Lambda))} + \|\varphi - \pi_{N,y}^{\gamma,0}\pi_{N,x}^{\gamma,0}\varphi\|_{L^2(\Lambda;H^\nu(\Lambda))}. \end{aligned} \tag{29}$$

By using the triangle inequality and estimate (28), we get

$$\begin{aligned} &\|\varphi - \pi_{N,y}^{\gamma,0}\pi_{N,x}^{\gamma,0}\varphi\|_{H^\nu(\Lambda;L^2(\Lambda))} \\ \lesssim& \|\varphi - \pi_{N,y}^{\gamma,0}\varphi\|_{H^\nu(\Lambda;L^2(\Lambda))} + \|\pi_{N,y}^{\gamma,0}\varphi - \pi_{N,y}^{\gamma,0}\pi_{N,x}^{\gamma,0}\varphi\|_{H^\nu(\Lambda;L^2(\Lambda))} \\ \lesssim& N^{\nu-\sigma}\|\varphi\|_{H^\nu(\Lambda;H^{\sigma-\nu}(\Lambda))} + \|\pi_{N,y}^{\gamma,0}\big(\varphi - \pi_{N,x}^{\gamma,0}\varphi\big)\|_{H^\nu(\Lambda;L^2(\Lambda))} \\ \lesssim& N^{\nu-\sigma}\|\varphi\|_{H^\nu(\Lambda;H^{\sigma-\nu}(\Lambda))} + \|\varphi - \pi_{N,x}^{\gamma,0}\varphi\|_{H^\nu(\Lambda;L^2(\Lambda))} \\ \lesssim& N^{\nu-\sigma}\|\varphi\|_{H^\nu(\Lambda;H^{\sigma-\nu}(\Lambda))} + N^{\nu-\sigma}\|\varphi\|_{H^\sigma(\Lambda;L^2(\Lambda))}. \end{aligned}$$

Furthermore, using (6) and (7) gives

$$\|\varphi - \pi_{N,y}^{\gamma,0}\pi_{N,x}^{\gamma,0}\varphi\|_{H^\nu(\Lambda;L^2(\Lambda))} \lesssim N^{\nu-\sigma}\|\varphi\|_\sigma. \tag{30}$$

Similarly, we have

$$\|\varphi - \pi_{N,y}^{\gamma,0}\pi_{N,x}^{\gamma,0}\varphi\|_{L^2(\Lambda;H^\nu(\Lambda))} \lesssim N^{\nu-\sigma}\|\varphi\|_\sigma. \tag{31}$$

Then we bring (30) and (31) into (29) to get (27). The case $d = 3$ can be proved in a similar way. □

In the next lemma, we give a polynomial approximation result for divergence-free functions. Note that a similar approximation result has been provided by Landriani & Vandeven [23] for divergence-free functions. The following lemma extends this result in the following senses: 1) in 2D case, we will give a different proof allowing to obtain the optimal error estimate under a less restrictive condition; 2) in 3D case, the $H^1$-estimate given in [23] is generalized to $H^\alpha$-estimate for divergence-free functions.

**Lemma 4.2.** *Let $s \geq \alpha$ when $d = 2$ and $s \geq 3$ when $d = 3$. Then for any divergence-free function $\boldsymbol{v} \in H^s(\Omega)^d \cap X$, the following estimate holds:*

$$\inf_{\boldsymbol{v}_N \in K_N} \|\boldsymbol{v} - \boldsymbol{v}_N\|_X \lesssim N^{\alpha-s}\|\boldsymbol{v}\|_s. \tag{32}$$

*Proof.* (i) The case $d = 2$. First we recall that [18] for any $\boldsymbol{v} \in H_0^\alpha(\Omega)^2$, there exists a stream function $\psi \in H_0^{\alpha+1}(\Omega)$ such that $\boldsymbol{v} = \operatorname{curl}\psi$. Moreover, if $\boldsymbol{v}$ belongs to $H^s(\Omega)^2, s \geq \alpha$, then we have $\psi \in H^{s+1}(\Omega)$, and

$$\|\psi\|_{s+1} \lesssim \|\boldsymbol{v}\|_s. \tag{33}$$

Let $\Pi_{s+1,N}^{\alpha+1,0}$ be the operator from $H^{s+1}(\Omega) \cap H_0^{\alpha+1}(\Omega)$ onto $\mathbb{P}_N(\Omega) \cap H_0^{\alpha+1}(\Omega)$, constructed in Lemma 4.1 with $p = s+1$ and $\gamma = \alpha+1$. Then we have $\operatorname{curl}\Pi_{s+1,N}^{\alpha+1,0}\psi \in K_N$, and, using (27) and (33),

$$\begin{aligned}\inf_{\boldsymbol{v}_N \in \mathrm{K}_N} \|\boldsymbol{v} - \boldsymbol{v}_N\|_X &\leq \|\operatorname{curl}\psi - \operatorname{curl}\Pi_{s+1,N}^{\alpha+1,0}\psi\|_X \leq \|\operatorname{curl}\psi - \operatorname{curl}\Pi_{s+1,N}^{\alpha+1,0}\psi\|_\alpha \\ &\leq \|\psi - \Pi_{s+1,N}^{\alpha+1,0}\psi\|_{\alpha+1} \lesssim N^{\alpha-s}\|\psi\|_{s+1} \lesssim N^{\alpha-s}\|\boldsymbol{v}\|_s.\end{aligned}$$

(ii) Case $d = 3$. It has been proved in [23] that there exists an operator $\wp_{2,N}^i$ such that for all $\boldsymbol{v} \in H^s(\Omega)^d \cap X$ with $s > 3$, $\wp_{2,N}^i\boldsymbol{v}$ is a divergence free polynomial of degree $\leq N$ in the $i$ variable with $i = x, y, z$, and

$$\|\boldsymbol{v} - \wp_{2,N}^i\boldsymbol{v}\|_\alpha \lesssim N^{\alpha-s}\|\boldsymbol{v}\|_s. \tag{34}$$

Now let $\pi_{\alpha,N}^{i,\mathrm{div}}, i = x, y, z$, be the orthogonal projection operator for the inner product of $X$ onto the divergence-free subspace of $H_0^\alpha(\Omega)^3$, which is polynomial of degree $N$ in the $i$ variable. Then we approximate $\boldsymbol{v}$ by $\Pi_{\alpha,N}^{\mathrm{div}}\boldsymbol{v} := \pi_{\alpha,N}^{x,\mathrm{div}}\pi_{\alpha,N}^{y,\mathrm{div}}\pi_{\alpha,N}^{z,\mathrm{div}}\boldsymbol{v}$. It follows from the orthogonality of $\pi_{\alpha,N}^{i,\mathrm{div}}$ and the triangular inequality:

$$\begin{aligned}\inf_{\boldsymbol{v}_N \in K_N} \|\boldsymbol{v} - \boldsymbol{v}_N\|_X &\lesssim \|\boldsymbol{v} - \Pi_{\alpha,N}^{\mathrm{div}}\boldsymbol{v}\|_X = \|\boldsymbol{v} - \pi_{\alpha,N}^{x,\mathrm{div}}\pi_{\alpha,N}^{y,\mathrm{div}}\pi_{\alpha,N}^{z,\mathrm{div}}\boldsymbol{v}\|_\alpha \\ &\lesssim \|\boldsymbol{v} - \pi_{\alpha,N}^{x,\mathrm{div}}\boldsymbol{v}\|_\alpha + 2\|\boldsymbol{v} - \pi_{\alpha,N}^{y,\mathrm{div}}\boldsymbol{v}\|_\alpha + 3\|\boldsymbol{v} - \pi_{\alpha,N}^{z,\mathrm{div}}\boldsymbol{v}\|_\alpha \\ &\lesssim \|\boldsymbol{v} - \wp_{2,N}^x\boldsymbol{v}\|_\alpha + 2\|\boldsymbol{v} - \wp_{2,N}^y\boldsymbol{v}\|_\alpha + 3\|\boldsymbol{v} - \wp_{2,N}^z\boldsymbol{v}\|_\alpha \\ &\lesssim N^{\alpha-s}\|\boldsymbol{v}\|_s.\end{aligned}$$

This proves the desired result. □

We are now at a position to derive the error estimate for the numerical solution.

**Theorem 4.2.** *Let $s, \sigma$, and $\gamma$ be positive real numbers, $s \geq \alpha$ when $d = 2$ and $s \geq 3$ when $d = 3$. Assume that the solution $(\boldsymbol{u}, p)$ of the continuous problem (14)-(15) belongs to $H^s(\Omega)^d \times H^\sigma(\Omega)$, and $\boldsymbol{f} \in H^\gamma(\Omega)^d$. Then the spectral approximation solution $(\boldsymbol{u}_N, p_N)$ of (20)-(21) satisfies the following error estimate:*

$$\|\boldsymbol{u} - \boldsymbol{u}_N\|_X + \beta_N\|p - p_N\|_0 \lesssim N^{4-4\alpha}(N^{\alpha-s}\|\boldsymbol{u}\|_s + N^{-\sigma}\|p\|_\sigma + N^{-\gamma}\|\boldsymbol{f}\|_\gamma), \tag{35}$$

*where $\beta_N$ is the Inf-Sup constant given in Theorem 4.1.*

*Proof.* Using a standard approximation result for the saddle point problem, we get

$$\begin{aligned}\|\boldsymbol{u} - \boldsymbol{u}_N\|_X + \frac{\beta_N}{1+\gamma_N}\|p - p_N\|_0 \lesssim \frac{1}{\delta_N}\Bigg(&\inf_{\boldsymbol{v}_N \in K_N \cap \mathbb{P}_{N-1}(\Omega)^d} \|\boldsymbol{u} - \boldsymbol{v}_N\|_X \\ &+ \inf_{q_N \in M_N} \|p - q_N\|_0 + \sup_{\boldsymbol{w}_N \in X_N} \frac{(f, \boldsymbol{w}_N) - (f, \boldsymbol{w}_N)_N}{\|\boldsymbol{w}_N\|_X}\Bigg),\end{aligned}$$

where $\delta_N$ is the discrete coercivity constant given in (26). Then the estimate (35) follows directly from Lemma 4.2 and some standard approximation results (see, e.g., [9]). □

**Remark 4.1.** *The error estimate in* (35) *is not optimal. This is due to the loss of the uniform coercivity of* $a_N(\cdot,\cdot)$ *in* $K_N \times K_N$ *given in* (26)*. The cause of this loss is that in the discrete case the divergence of the velocity field is not strictly zero, so that an inverse inequality had to be applied to control the divergence of the discrete velocity. Theoretically, this difficulty can be overcome by adding the divergence term* $(\nabla \cdot \boldsymbol{u}_N, \nabla \cdot \boldsymbol{v}_N)_N$ *to the bilinear form* $a_N(\boldsymbol{u}_N, \boldsymbol{v}_N)$*. However the drawback of this formulation is that the different components are coupled in the velocity equation, making the computation more expensive. Our numerical tests have shown much better coercivity constant* $\delta_N$ *than that the theoretical estimation provides without the divergence term. This is probably due to the fact that in most practical cases the divergence of the discrete velocity is very small.*

## 5. Numerical results

**5.1. Implementation.** We first give the implementation detail for the problem (22)-(23) in 2D. Let $h^{s,\sigma}_{N,i}(x)$ and $l^{s,\sigma}_{N,i}(x), i = 0, \cdots, N$, denote the Lagrangian polynomials associated to the $N+1$ Jacobi Gauss-Lobatto points and $N+1$ Jacobi Gauss points with respect to the weight $w(x) = (1-x)^s(1+x)^\sigma$ respectively. We express the velocity components $u^r_N, r = 1, 2$ in term of the Lagrangian polynomials based on the Legendre-Gauss-Lobatto points ($s = \sigma = 0$):

$$u^r_N(x, y) = \sum_{i,j=1}^{N-1} u^r_N(\xi_i, \xi_j) h^{0,0}_{N,i}(x) h^{0,0}_{N,j}(y), \quad r = 1, 2. \tag{36}$$

In the above expression the indices $i, j = 0$ and $i, j = N$ are eliminated due to the Dirichlet boundary condition on the velocity. Let $\underline{\boldsymbol{u}}_N$ denotes the velocity unknowns vector which represents the values of all the components at the nodes $(\xi^{0,0}_{N,i}, \xi^{0,0}_{N,j})_{1\le i,j\le N-1}$. The pressure $p_N$ is represented at the Legendre-Gauss nodes by

$$p_N(x, y) = \sum_{i,j=0}^{L} p_N(\eta^{0,0}_{L,i}, \eta^{0,0}_{L,j}) l^{0,0}_{L,i}(x) l^{0,0}_{L,j}(y), \tag{37}$$

where $L = N - 2$. Note that the pressure is computed up to an additive constant. We use $\underline{p}_N$ to mean the pressure unknowns vector representing the values of $p_N$ at the nodes $(l^{0,0}_{L,i}, l^{0,0}_{L,j})_{0\le i,j\le L}$.

We insert the expressions (36) and (37) into (20)–(21) and take the test functions $\boldsymbol{v}_N$ and $q_N$ to be the Lagrangian nodal basis functions associated to the Gauss-Lobatto-Legendre and Gauss-Legendre nodes respectively, then we obtain the linear system under the following form:

$$\mathbf{A}^\alpha_N \underline{\mathbf{u}}_N + \mathbf{D}^T_N \underline{p}_N = \mathbf{B}_N \underline{\mathbf{f}}_N, \tag{38}$$

$$\mathbf{D}_N \underline{\mathbf{u}}_N = 0, \tag{39}$$

where $\underline{\mathbf{f}}_N$ is a vector representation of the data $\mathbf{f}$. $\mathbf{A}^\alpha_N$, $\mathbf{D}_N$, and $\mathbf{B}_N$ are block-diagonal matrices with $d$ blocks each. The blocks of $\mathbf{A}^\alpha_N$ are the discrete fractional Laplace operators, and those of $\mathbf{D}_N$ are associated to the different components of the discrete gradient operators. $\mathbf{B}_N$, usually called mass matrices, are diagonal.

The main difficulty in the generation of the linear system is in computing the stiffness matrices $\mathbf{A}^\alpha_N$ involving fractional derivatives. That is, we have to deal with the following inner products in $x$ direction (same in $y$):

$$\left({}_{-1}^{\;C}D_x^\alpha h_{N,i}^{0,0}(x), {}_xD_1^\alpha h_{N,j}^{0,0}(x)\right), \quad \left({}_x^CD_1^\alpha h_{N,i}^{0,0}(x), {}_xD_1^\alpha h_{N,j}^{0,0}(x)\right), \tag{40}$$

$$\left({}_x^CD_1^\alpha h_{N,i}^{0,0}(x), {}_{-1}D_x^\alpha h_{N,j}^{0,0}(x)\right), \quad \left({}_{-1}^{\;C}D_x^\alpha h_{N,i}^{0,0}(x), {}_{-1}D_x^\alpha h_{N,j}^{0,0}(x)\right). \tag{41}$$

A formula allowing exact evaluation of the above inner products under homogeneous boundary condition was given in [25]. Here we choose an alternative method using Jacobi polynomials. To this end, we take $\rho = 1-\alpha, s = 0, \sigma = 0$ in (1) to get

$$\begin{aligned}{}_{-1}^{\;C}D_x^\alpha h_{N,i}^{0,0}(x) &= {}_{-1}I_x^{1-\alpha} h_{N,i}^{0,0\,\prime}(x) \\ &= {}_{-1}I_x^{1-\alpha} \sum_{n=0}^N c_n^i J_n^{0,0}(x) = (1+x)^{1-\alpha} \sum_{n=0}^N \bar{c}_n^i J_n^{\alpha-1,1-\alpha}(x),\end{aligned} \tag{42}$$

where $\{c_n^i\}$ are the expansion coefficients of $h_{i,N}^{0,0\,\prime}$ in terms of $J_n^{0,0}$, and $\bar{c}_n^i = \frac{\Gamma(n+1)}{\Gamma(n+2-\alpha)} c_n^i$. $c_n^i$ can be obtained by using the formulas given in [36]. Similarly, using (2) we have

$$\begin{aligned}{}_x^CD_1^\alpha h_{N,i}^{0,0}(x) &= -\,{}_xI_1^{1-\alpha} h_{N,i}^{0,0\,\prime}(x) \\ &= -\,{}_xI_1^{1-\alpha} \sum_{n=0}^N c_n^i J_n^{0,0}(x) = -(1-x)^{1-\alpha} \sum_{n=0}^N \bar{c}_n^i J_n^{1-\alpha,\alpha-1}(x).\end{aligned} \tag{43}$$

For the RL fractional derivatives of the Lagrangian polynomials, with the help of (3) and (4), we have

$${}_{-1}D_x^\alpha h_{N,j}^{0,0}(x) = {}_{-1}D_x^\alpha \sum_{n=0}^N r_n^j J_n^{0,0}(x) = (1+x)^{-\alpha} \sum_{n=0}^N \bar{r}_n^j J_n^{\alpha,-\alpha}(x), \tag{44}$$

$${}_xD_1^\alpha h_{N,j}^{0,0}(x) = {}_xD_1^\alpha \sum_{n=0}^N r_n^j J_n^{0,0}(x) = (1-x)^{-\alpha} \sum_{n=0}^N \bar{r}_n^j J_n^{-\alpha,\alpha}(x), \tag{45}$$

where $\bar{r}_n^j = \frac{\Gamma(n+1)}{\Gamma(n+1-\alpha)} r_n^j$. Then we derive from combining (42) and (45),

$$\begin{aligned}&\left({}_{-1}^{\;C}D_x^\alpha h_{N,i}^{0,0}(x), {}_xD_1^\alpha h_{N,j}^{0,0}(x)\right) \\ &= \int_{-1}^1 (1-x)^{-\alpha}(1+x)^{1-\alpha} \left(\sum_{n=0}^N \bar{c}_n^i J_n^{\alpha-1,1-\alpha}\right)\left(\sum_{n=0}^N \bar{r}_n^j J_n^{-\alpha,\alpha}\right) dx \\ &= \int_{-1}^1 (1-x)^{-\alpha}(1+x)^{1-\alpha} \left(\sum_{n=0}^N \hat{c}_n^i h_{N,n}^{-\alpha,1-\alpha}\right)\left(\sum_{n=0}^N \hat{r}_n^j h_{N,n}^{-\alpha,1-\alpha}\right) dx \\ &= \sum_{n=0}^N \hat{c}_n^i \hat{r}_n^j \omega_{N,n}^{-\alpha,1-\alpha}.\end{aligned}$$

Similarly we have,

$$\begin{aligned}
&\left({}_x^C D_1^\alpha h_{N,i}^{0,0}(x), {}_{-1}D_x^\alpha h_{N,j}^{0,0}(x)\right)\\
&= \int_{-1}^{1} (1-x)^{1-\alpha}(1+x)^{-\alpha} \left(\sum_{n=0}^{N} \tilde{c}_n^i h_{N,n}^{1-\alpha,-\alpha}\right)\left(\sum_{n=0}^{N} \tilde{r}_n^j h_{N,n}^{1-\alpha,-\alpha}\right) dx\\
&= \sum_{n=0}^{N+1} \tilde{c}_n^i \tilde{r}_n^j \omega_{N,n}^{1-\alpha,-\alpha};\\
&\left({}_{-1}^{C}D_x^\alpha h_{N,i}^{0,0}(x), {}_{-1}D_x^\alpha h_{N,j}^{0,0}(x)\right)\\
&= \int_{-1}^{1} (1+x)^{1-2\alpha} \left(\sum_{n=0}^{N} \check{c}_n^i h_{N,n}^{0,1-2\alpha}\right)\left(\sum_{n=0}^{N} \check{r}_n^{l,j} h_{N,n}^{0,1-2\alpha}\right) dx\\
&= \sum_{i=0}^{N} \check{c}_n^i \check{r}_n^j \omega_{N,n}^{0,1-2\alpha};\\
&\left({}_x^C D_1^\alpha h_{N,i}^{0,0}(x), {}_x D_1^\alpha h_{N,j}^{0,0}(x)\right)\\
&= \int_{-1}^{1} (1-x)^{1-2\alpha} \left(\sum_{n=0}^{N} \breve{c}_n^i h_{N,n}^{1-2\alpha,0}\right)\left(\sum_{n=0}^{N} \breve{r}_n^j h_{N,n}^{1-2\alpha,0}\right) dx\\
&= \sum_{n=0}^{N} \breve{c}_n^i \breve{r}_n^j \omega_{N,n}^{1-2\alpha,0}.
\end{aligned}$$

The $\hat{c}_n^i, \hat{r}_n^j, \bar{c}_n^i, \check{r}_n^j, \tilde{c}_n^i, \tilde{c}_n^j, \check{c}_n^i, \breve{r}_n^j$ are expansion coefficients from spectral space to physical space with respect to corresponding weight.

A classical method to deal with the discrete saddle point problem like (38)-(39) is the so-called Uzawa algorithm, which we will adopt here. The algorithm makes use of the following idea. A block Gaussian elimination is performed on the first equation (38) to decouple the pressure and the velocity. Then the pressure is solved from:

$$\mathbf{S}_\alpha \underline{p}_N = \mathbf{D}_N \mathbf{A}_N^{-\alpha} \mathbf{B}_N\, \underline{\mathbf{f}}_N, \quad \text{with } \mathbf{S}_\alpha = \mathbf{D}_N \mathbf{A}_N^{-\alpha} \mathbf{D}_N^T. \tag{46}$$

Once the pressure $\underline{p}_N$ is known, the velocity $\underline{\mathbf{u}}_N$ is solved from (38).

The matrix $\mathbf{S}_\alpha$ is also known as Uzawa matrix. It is of dimension $(N-1)^2$, full, symmetric, and semi-definite. In the classcial case, that is $\alpha = 1$, the pressure equation (46) used to be solved by a preconditioned conjugate gradient (PCG) procedure with the mass matrix $\mathbf{B}_N$ as the preconditioner [9, 29]. However in the current case, i.e., when $\alpha < 1$, the mass matrix $\mathbf{B}_N$ maybe no longer suitable as a good preconditioner. One of the main goals of the following numerical tests is to investigate the property of the preconditioned matrix $\mathbf{B}_N^{-1}\mathbf{S}_\alpha$, and attempt to make better choices for preconditioners. Note that in solving (46) by PCG procedure, each iteration requires the inversion of the fractional Laplace operator $\mathbf{A}_N^\alpha$. In our calculation performed hereafter, the inversion of $\mathbf{A}_N^\alpha$ will be realized by a fast diagonalization method, similar to that for the classical Laplace operator; see, e.g., [27].

**5.2. Numerical results.** The first numerical investigation is concerned with the *Inf-Sup* constant predicted by Theorem 4.1. It has been known (see, e.g., [29]) that *Inf-Sup* constant for the traditional Stokes equation is linked to the smallest eigenvalue of the preconditioned Uzawa operator. Precisely, it was proved in [29] that $\lambda_{\min}^{\alpha} \cong \beta_N^2$ when $\alpha = 1$, where $\lambda_{\min}^{\alpha}$ is the smallest eigenvalue of $\mathbf{B}_N^{-1}\mathbf{S}_\alpha$. Here we want to show that the relationship $\lambda_{\min}^{\alpha} \cong \beta_N^2$ remains true for $1/2 < \alpha < 1$ if the bilinear form $a_N(\mathbf{u}, \mathbf{v})$ is replaced by $a_N(\mathbf{u}, \mathbf{v}) + (\nabla \cdot \mathbf{u}, \nabla \cdot \mathbf{v})_N$. In fact, we have

$$\lambda_{\min}^{\alpha} = \inf_{p \in M_N} ((\nabla_N \cdot \mathcal{A}_N^{-\alpha} \nabla_N^T) p, p)_N. \quad (p, p)_N = 1, \tag{47}$$

where the operators $\nabla_N^T$ and $\mathcal{A}_N^{\alpha}$ are defined by:

$$(\mathbf{v}, \nabla_N^T p) := (\nabla \cdot \mathbf{v}, p)_N, \quad \forall \mathbf{v} \in X_N, \forall p \in M_N,$$
$$(\mathcal{A}_N^{\alpha} \mathbf{u}, \mathbf{v}) := a_N(\mathbf{u}, \mathbf{v}) + (\nabla \cdot \mathbf{u}, \nabla \cdot \mathbf{v})_N, \quad \forall \mathbf{u}, \mathbf{v} \in X_N.$$

We also define the inner product

$$((\mathbf{u}, \mathbf{v}))_N := a_N(\mathbf{u}, \mathbf{v}) + (\nabla \cdot \mathbf{u}, \nabla \cdot \mathbf{v})_N, \quad \forall \mathbf{u}, \mathbf{v} \in X_N,$$

then

$$\beta_N \cong \inf_{p \in M_N} \sup_{\mathbf{v} \in X_N} \frac{-(\nabla \cdot \mathbf{v}, p)_N}{((\mathbf{v}, \mathbf{v}))_N^{1/2}}, \quad (p, p)_N = 1.$$

Let $\tilde{\mathbf{u}} \in X_N$ be the solution of the problem

$$\tilde{\mathbf{u}} = -\mathcal{A}_N^{-\alpha} \nabla_N^T p, \tag{48}$$

then using the Cauchy-Schwarz inequality gives

$$\frac{-(\nabla \cdot \mathbf{v}, p)_N}{((\mathbf{v}, \mathbf{v}))_N^{1/2}} = \frac{((\tilde{\mathbf{u}}, \mathbf{v}))_N}{((\mathbf{v}, \mathbf{v}))_N^{1/2}} \leq ((\tilde{\mathbf{u}}, \tilde{\mathbf{u}}))_N^{1/2}, \ \forall \mathbf{v} \in X_N.$$

The above inequality becomes equality iff $\tilde{\mathbf{u}}$ and $\mathbf{v}$ are colinear, this lead from (48) to

$$\sup_{\mathbf{v} \in X_N} \frac{-(\nabla \cdot \mathbf{v}, p)_N}{((\mathbf{v}, \mathbf{v}))_N^{1/2}} = ((\tilde{\mathbf{u}}, \tilde{\mathbf{u}}))_N^{1/2} = ((\nabla_N \cdot \mathcal{A}_N^{-\alpha} \nabla_N^T) p, p)_N^{1/2}.$$

So that the inf-sup condition satisfies

$$\beta_N \cong \inf_{p \in M_N} ((\nabla_N \cdot \mathcal{A}_N^{-\alpha} \nabla_N^T) p, p)_N^{\frac{1}{2}}, \quad (p, p)_N = 1.$$

Now we recalling (47), we have $\lambda_{\min}^{\alpha} \cong \beta_N^2$.

In Figure 1 we present the eigenvalue distributions of $\mathbf{B}_N^{-1}\mathbf{S}_\alpha$ for several values of $\alpha$ for the 2-dimensional case. The results for the 3-dimensional case is shown in Figure 2. We first observe that the maximum eigenvalues corresponding to $\alpha = 1$ remain 1 for all $N$, which is a fact well-known. For fractional cases the maximum eigenvalue increases along with the growth of polynomial degree, and the growth rates are almost same for the 2-dimensional and the 3-dimensional cases. Figure 3 depicts the variations of $\lambda_{\min}^{\alpha}$ versus $N$ for $\alpha \in \{0.55, 0.75, 0.95, 1\}$. We observe, as expected from Theorem 4.1, that the inf-sup condition of the fractional Stokes equation decreases slowly as $N$ increases, but no worse than $N^{-0.5}$, which corresponds to the traditional case $\alpha = 1$.

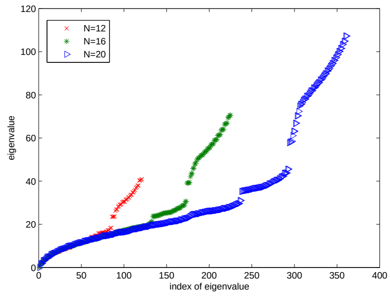


(A) $\alpha = 0.55$

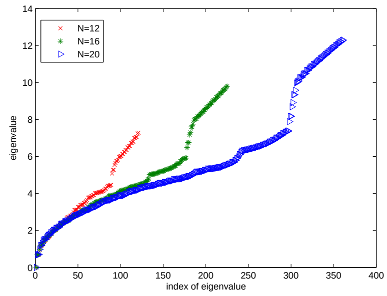


(B) $\alpha = 0.75$

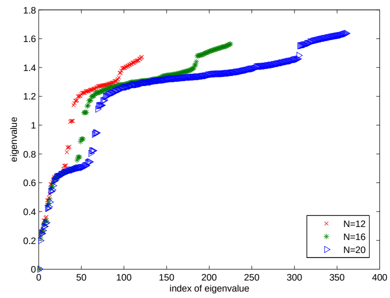


(C) $\alpha = 0.95$

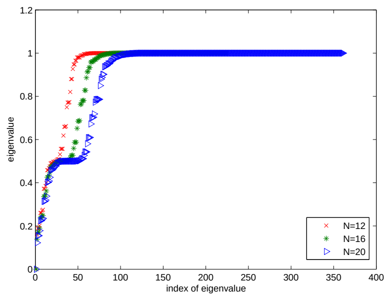


(D) $\alpha = 1.00$

FIGURE 1. Eigenvalues for different $\alpha$ in two dimensional case.

We now present some numerical tests for the validation of the error estimates. In particular, we look at the steady Stokes problem with the following analytical solutions for $d = 2$:

$$\text{Test 1} \qquad \mathbf{u} = \begin{pmatrix} \cos(\pi x)\cos(\pi y) \\ \sin(\pi x)\sin(\pi y) \end{pmatrix}, \quad p = \sin(\pi(x+y));$$

$$\text{Test 2} \qquad \mathbf{u} = \begin{pmatrix} \sin^2(\pi x)\sin(\pi y) \\ 2\sin(2\pi x)\cos^2(\frac{\pi y}{2}) \end{pmatrix}, \quad p = x^\gamma \sin(\pi x)\sin(\pi y);$$

$$\text{Test 3} \qquad \mathbf{u} = \begin{pmatrix} \pi x^\gamma \sin^2(\pi x)\sin(\pi y) \\ 2[\pi x^\gamma \sin(2\pi x) + \gamma x^{\gamma-1}\sin^2(\pi x)]\cos^2(\frac{\pi y}{2}) \end{pmatrix},$$
$$p = \sin(\pi(x+y));$$

where $\gamma$ is a given constant. The error behavior is investigated by first computing the $\mathbb{P}_N \times \mathbb{P}_{N-2}$–spectral approximation solutions for a sequence of $N$, then measuring the gap in term of suitable norms between the computed and the exact solutions.

In Figure 4(A)(B) we plot the evolution, in a semi-log scale, of the $H^\alpha$-velocity error and the $L^2$-pressure error respectively as functions of the polynomial degree $N$ for $d = 2$. The exponential decay of the errors, due to the smoothness of both $\mathbf{u}$ and $p$ in Test 1, is clearly obtained as predicted by the theoretical estimation. Figure 4(C) shows the pressure error decay for the non-smooth pressure solution of different regularities, characterized by the parameter $\gamma$, given in Test 2. The fact that the error curves are straight lines in the log-log representation

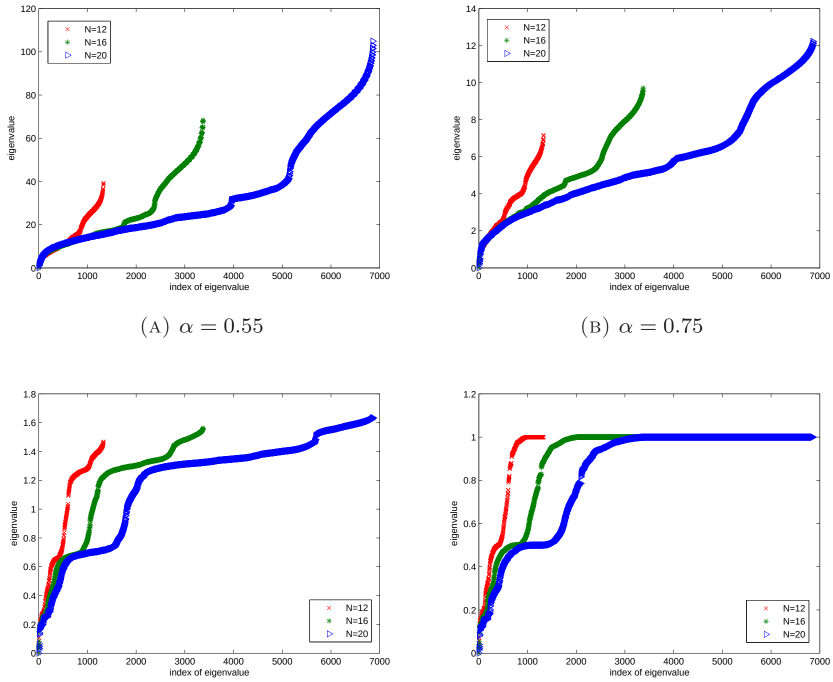


(A) $\alpha = 0.55$ (B) $\alpha = 0.75$

(C) $\alpha = 0.95$ (D) $\alpha = 1.00$

FIGURE 2. Eigenvalues for different $\alpha$ in three dimensional case.

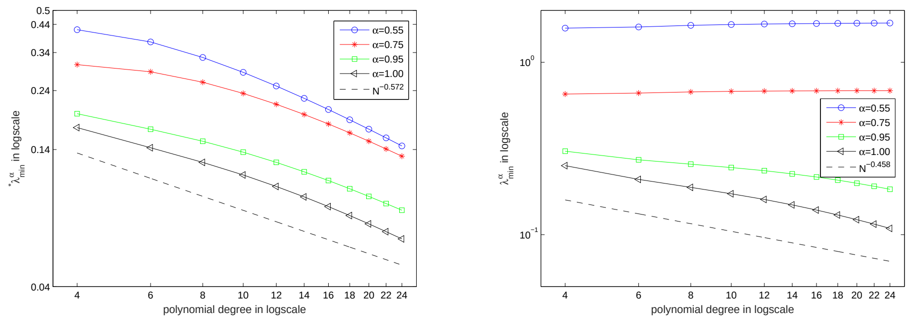


(A) (B)

FIGURE 3. $\lambda^{\alpha}_{\min}$ with divergence term (left), $\lambda^{\alpha}_{\min}$ without divergence term (right) as a function of the polynomial degree in two dimensional case.

indicates that only algebraic accuracy is obtained. A closer look at the figure shows that the convergence rates are approximately $N^{-4.667}, N^{-6.667}, N^{-8.667}$ respectively (For given $\gamma = \frac{11}{3}, \frac{17}{3}, \frac{23}{3}$, the pressure $p \in H^{5.167}, H^{7.167}H^{9.167}$, then the *slop* $= -\{5.167, 7.167, 9.167\} + 0.5$), which is better than the estimate given in

(35). As explained in Remark 4.1, the theoretical error estimate given in Theorem 4.2 does not reflect actual error behavior, and the coupled bilinear form is not really necessary for obtaining more accurate numerical solutions. We investigate by using Test 3 the error behavior when the exact velocity solution is non-smooth. The corresponding result is plotted in Figure 4(D), in which the error evolution with respect to $N$ is presented for the solution given in Test 3 with different values for the regularity parameter $\gamma$. It is observed that the error decay rate is close to $N^{-4.083,-6.083,-8.083}$ (for given $\gamma = \frac{10}{3}, \frac{16}{3}, \frac{22}{3}$, the velocity $\mathbf{u} \in H^{4.833}, H^{6.833}, H^{8.833}$, then the *slop* $= \alpha - \{4.833, 6.833, 8.833\}$), which is once again better than the one predicted by Theorem 4.2.

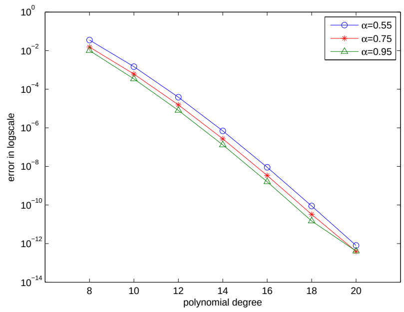


(A) Velocity error decay for Test 1

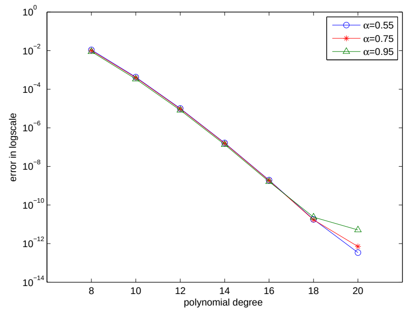


(B) Pressure error decay for Test 1

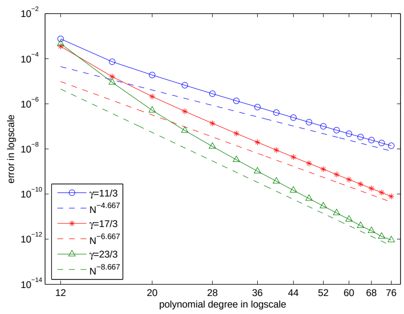


(C) Pressure error for Test 2 with $\alpha = 0.75$

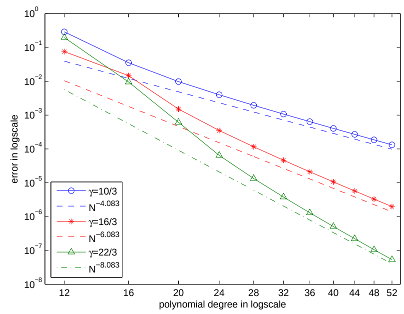


(D) Velocity error for Test 3 with $\alpha = 0.75$

FIGURE 4. Error as a function of polynomial.

Now we turn to investigate suitable preconditioners for PCG method to solve (46). It has been known for the traditional Stokes operator that the mass matrix $\mathbf{B}_M$ is an efficient preconditioner for the Uzawa matrix $\mathbf{S}_1$. However, our numerical experiments show that the efficiency decreases when the fractional order $\alpha$ decreases. This can be seen in Table 1 and Table 2, where the iteration numbers as functions of $N$ required by PCG for reaching the convergence are listed for several values of $\alpha$. That is, smaller is $\alpha$, faster is the growth of the required iteration numbers when $N$ increases. This motivates us to construct an alternative preconditioner. Naturally, the $1-\alpha$ order fractional Laplacian $\Delta^{1-\alpha}$ defined below is a

TABLE 1. Number of iterations for different $\alpha$ ($d = 2$).

| | $\alpha = 1.1$ | | $\alpha = 1.5$ | | $\alpha = 1.9$ | | $\alpha = 2.0$ |
|---|---|---|---|---|---|---|---|
| $N$ | $\mathbf{B}_M$ | $\Delta^{1-\alpha}$ | $\mathbf{B}_M$ | $\Delta^{1-\alpha}$ | $\mathbf{B}_M$ | $\Delta^{1-\alpha}$ | $\mathbf{B}_M$ |
| 8 | 13 | 13 | 13 | 13 | 12 | 12 | 10 |
| 16 | 34 | 29 | 25 | 20 | 17 | 16 | 13 |
| 24 | 51 | 34 | 30 | 21 | 18 | 18 | 15 |
| 32 | 68 | 36 | 34 | 22 | 18 | 18 | 15 |
| 40 | 82 | 37 | 38 | 23 | 19 | 18 | 15 |
| 48 | 97 | 37 | 41 | 23 | 19 | 19 | 15 |
| 56 | 111 | 38 | 44 | 24 | 20 | 19 | 16 |
| 64 | 125 | 39 | 44 | 24 | 20 | 19 | 16 |

TABLE 2. Number of iterations for different $\alpha$ ($d = 3$).

| | $\alpha = 1.1$ | | $\alpha = 1.5$ | | $\alpha = 1.9$ | | $\alpha = 2.0$ |
|---|---|---|---|---|---|---|---|
| $N$ | $\mathbf{B}_M$ | $\Delta^{1-\alpha}$ | $\mathbf{B}_M$ | $\Delta^{1-\alpha}$ | $\mathbf{B}_M$ | $\Delta^{1-\alpha}$ | $\mathbf{B}_M$ |
| 8 | 29 | 47 | 28 | 30 | 25 | 26 | 24 |
| 16 | 55 | 75 | 41 | 44 | 30 | 33 | 27 |
| 24 | 77 | 93 | 47 | 49 | 33 | 30 | 26 |
| 32 | 95 | 89 | 54 | 45 | 25 | 26 | 21 |
| 40 | 115 | 69 | 59 | 35 | 24 | 25 | 20 |
| 48 | 134 | 68 | 57 | 35 | 24 | 24 | 20 |
| 56 | 152 | 69 | 60 | 35 | 25 | 24 | 20 |
| 64 | 170 | 64 | 63 | 35 | 25 | 24 | 20 |

choice:

$$\Delta^{1-\alpha} := \frac{1}{4}\sum_{j=1}^{d}\left(D_{x_j}^{1-\alpha} - {}_{x_j}D^{1-\alpha}\right)\left(D_{x_j}^{1-\alpha} - {}_{x_j}D^{1-\alpha}\right). \tag{49}$$

Note that the above definition differs from the one in (11) in the sense that the right hand side derivatives involved in (49) are all of RL type, while some of them are of Caputo type in (11). An another point worthy of mentioning is that no boundary condition is necessary to inverse the operator $\Delta^{1-\alpha}$ since it is done by solving the associated problem in the weak form in the space $H^{1-\alpha}(\Omega)^d$. As for the inversion of $\mathbf{A}_N^{\alpha}$, the $\Delta^{1-\alpha}$-preconditioning is realized by the fast diagonalization method.

We use the discrete $\Delta^{1-\alpha}$ operator as the preconditioner for the CG iteration, and test the efficiency of the PCG algorithm in solving (46). In the calculation we set the threshold $\epsilon = 10^{-8}$. The result, together with a comparison with $\mathbf{B}_M$-preconditioner, is given in Table 1 for 2D case and Table 2 for 3D case. The fact that the required iteration numbers for the $\Delta^{1-\alpha}$-PCG are almost independent of the polynomial $N$ and fractional order $\alpha$ clearly indicates the superiority of the $\Delta^{1-\alpha}$ over $\mathbf{B}_M$ as preconditioner.

## 6. Fractional Navier-Stokes equation

In this section, we consider a fractional Navier-Stokes equation in two-dimension, which can be regarded as a potential application of the fractional Stokes equation studied in the previous sections. Precisely, we consider the following equations:

$$\frac{\partial \mathbf{u}}{\partial t} - \nu\Delta^\alpha \mathbf{u} + (\mathbf{u}\cdot\nabla)\mathbf{u} + \nabla p = \mathbf{f}, \quad \text{in } \Omega\times[0,T], \tag{50}$$

$$\nabla\cdot\mathbf{u} = 0, \quad \text{in } \Omega\times[0,T], \tag{51}$$

$$\mathbf{u} = \mathbf{g}, \quad \text{on } \partial\Omega\times[0,T], \tag{52}$$

$$\mathbf{u}(\cdot, t=0) = \mathbf{u}_0, \quad \text{on } \Omega, \tag{53}$$

where $\nu = \frac{1}{Re}$, $Re$ is the Reynolds number. For the time discretization of the above equations, two approaches are possible: the semi-implicit method and projection method. The former will result in a Stokes-like equation at each time step, then the $\mathbb{P}_N - \mathbb{P}_{N-2}$ method combined with the Uzawa algorithm proposed previously can be applied to compute the full discrete solutions. Next we propose a projection method. Let us divide the time interval $[0,T]$ into $K$ subdivisions of length $\Delta t = \frac{T}{K}$, and denote $t^k = k\Delta t$ for $k = 0, 1, \ldots, K$. We compute two sequences $(\mathbf{u}^k)_{0\le k\le K}$ and $(p^k)_{0\le k\le K}$ in a recurrent way, which are approximations to $(u(\cdot,t^k))_{0\le k\le K}$ and $(p(\cdot,t^k))_{0\le k\le K}$ respectively. The algorithm is as follows: Set $\mathbf{u}^0 = \mathbf{u}_0$, then for $k\ge 0$ compute $(\tilde{\mathbf{u}}^{k+1}, \mathbf{u}^{k+1}, p^{k+1})$ by solving

$$\begin{cases} \dfrac{\tilde{\mathbf{u}}^{k+1} - \mathbf{u}^k}{\Delta t} - \nu\Delta^\alpha\tilde{\mathbf{u}}^{k+1} + (\mathbf{u}^k\cdot\Delta)\mathbf{u}^k + \nabla p^k = \mathbf{f}^{k+1}, & \text{in } \Omega, \\ \tilde{\mathbf{u}}^{k+1} = \mathbf{g}, & \text{on } \partial\Omega, \end{cases} \tag{54}$$

$$\begin{cases} \dfrac{\mathbf{u}^{k+1} - \tilde{\mathbf{u}}^{k+1}}{\Delta t} + \nabla\phi^{k+1} = 0, & \text{in } \Omega, \\ \nabla\cdot\mathbf{u}^{k+1} = 0, & \text{in } \Omega, \\ \mathbf{u}^{k+1} = \mathbf{g}, & \text{on } \partial\Omega, \end{cases} \tag{55}$$

$$p^{k+1} = \phi^{k+1} + p^k. \tag{56}$$

In (55), $\phi^{k+1}$ can be obtained by solving the following Poisson equation, subject to the homogeneous Neumann condition:

$$\begin{cases} -\Delta\phi^{k+1} = -\dfrac{\nabla\cdot\tilde{\mathbf{u}}^{k+1}}{\Delta t}, & \text{in } \Omega, \\ \dfrac{\partial\phi^{k+1}}{\partial n} = 0, & \text{on } \partial\Omega. \end{cases}$$

Notice that in order to improve the pressure accuracy, in a pressure correction projection method for the traditional Navier-Stokes equations, the pressure correction step (56) used to be replaced by

$$p^{k+1} = \phi^{k+1} + p^k - \nu\nabla\cdot\tilde{\mathbf{u}}^{k+1}.$$

However, in the fractional case doing so would not allow to obtain the desired improvement. This is due to the fact that the following identity does not hold for $1/2 < \alpha < 1$:

$$\nabla\cdot\Delta^\alpha\mathbf{u} = \Delta^\alpha\nabla\cdot\mathbf{u}.$$

Our numerical tests have confirmed this point.

By curiosity we use this fractional incompressible flow model and the proposed scheme to simulate the driven cavity flow, which is a well-known benchmark problem. The purpose is to investigate the effect of the fractional derivative on the flow behaviors, particularly on the vertex formation. The boundary conditions used in the simulation are shown in Figure 5. The discretization parameters are set to $\Delta t = 0.0001, N = M = 64$.

Figures 6-8 show the streamline of the flows for the Reynolds numbers 100, 400, and 1000 for a number of $\alpha$. It has been known that in the case $\alpha = 1$ the flows under the tested Reynolds numbers evolve into steady state. Our simulation has shown that this remains true in the subdiffusion regime with $0.5 < \alpha < 1$. The stopping criteria used in the calculations is:

$$\|\mathbf{u}_N^{k+1} - \mathbf{u}_N^k\|_0 \leq 10^{-7} \quad \text{or} \quad T \leq 1000.$$

We have some more observations from Figures 6-8:

- Smaller is the Reynolds number, lighter is the impact of the fractional order on the vortex structure.

- Unexpected vortexes appear in some region close to the domain boundary at higher Reynolds numbers. There are two possible explanations for this phenomena:

1) the convection term dominates the diffusion more easily with increasing Reynolds number in the subdiffusion regime;

2) the fractional Laplacian operator causes a numerical boundary layer, due to its non-local nature. This issue has been addressed in [38] for a fractional phase-field model for two-phase flows, and a variable-order fractional model has been proposed to overcome this difficulty.

Obviously these observations deserve further investigation in the future. In particular, it is interesting to consider a fractional model with $\alpha > 1$. Moreover, it is also an issue how the variable-order fractional phase-field model introduced in [38] can be extended to the incompressible Navier-Stokes equations.

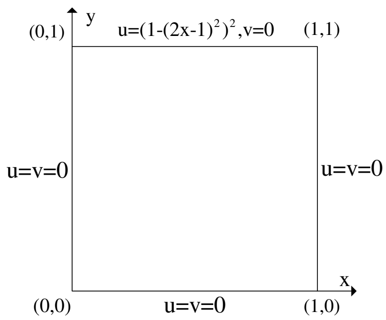


FIGURE 5. Boundary conditions for the driven cavity flow.

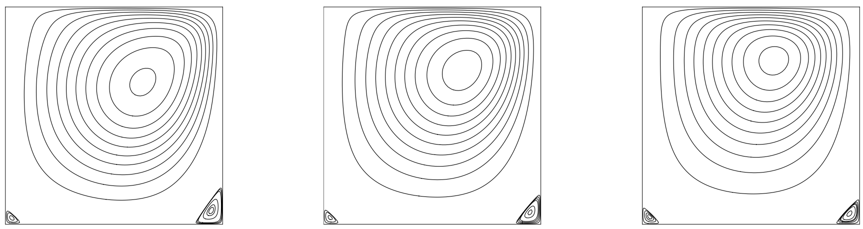

(A) $\alpha = 0.75$ (B) $\alpha = 0.85$ (C) $\alpha = 1.00$

FIGURE 6. Streamline at $Re = 100$.

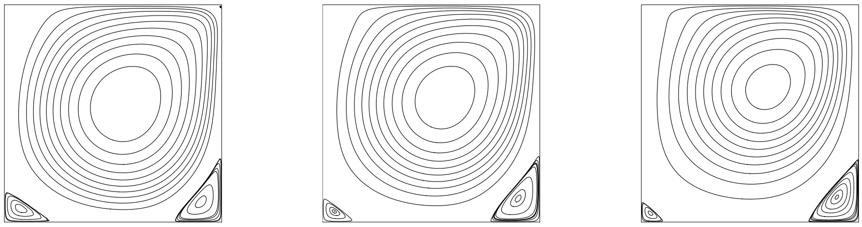

(A) $\alpha = 0.75$ (B) $\alpha = 0.85$ (C) $\alpha = 1.00$

FIGURE 7. Streamline at $Re = 400$.

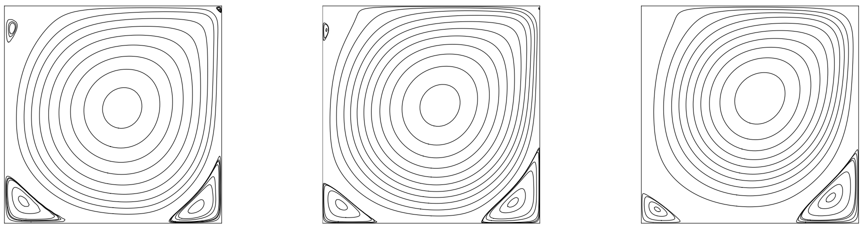

(A) $\alpha = 0.75$ (B) $\alpha = 0.85$ (C) $\alpha = 1.00$

FIGURE 8. Streamline at $Re = 1000$.

## 7. Concluding Remarks

This work represents the first attempt to consider a fractional Stokes equation, and develop a spectral approximation to this equation. First, we studied the well-posedness of the associated weak problem by introducing suitable functional spaces. The existence and uniqueness of the weak solution were established by applying the classical saddle-point theory. Then, using this variational framework, we proposed an efficient spectral method for numerical approximations of the weak solution. A detailed numerical analysis was carried to prove the well-posedness of the spectral discrete problem and derive useful error estimates for the numerical solutions. Some properties of the linear system are also investigated, together with a description of the fast solver. Several numerical examples are provided to confirm the theoretical results. Finally, an extension to the fractional incompressible Navier-Stokes equation was presented, along with corresponding numerical methods. Numerical simulations using this fractional model has provided some interesting results, which deserve further investigation in the future.

## Acknowledgments

This research is partially supported by NSF of China (Grant numbers 11471274, 11421110001, 51661135011, and 91630204).

## References

[1] R.A. Adams. Sobolev spaces. Acadmic Press, 1975.

[2] O.P. Agrawal. Formulation of Euler-Lagrange equations for fractional variational problems. Journal of Mathematical Analysis and Applications, 272:368–379, 2002.
[3] O.P. Agrawal. A general formulation and solution scheme for fractional optimal control problems. Nonlinear Dynamics, 38:191–206, 2004.
[4] D.A. Benson, R. Schumer, M.M. Meerschaert, and S.W. Wheatcraft. Fractional dispersion, Lévy motion, and the MADE tracer tests. Transport in Porous Media, 42(1):211–240, 2001.
[5] D.A. Benson, S.W. Wheatcraft, and M.M. Meerschaert. Application of a fractional advection-dispersion equation. Water Resources Research, 36(6):1403–1412, 2004.
[6] D.A. Benson, S.W. Wheatcraft, and M.M. Meerschaert. The fractional-order governing equation of Lévy motion. Water Resources Research, 36:1413–1423, 2006.
[7] C. Bernardi, M. Dauge, and Y. Maday. Polynomials in the sobolev world. Numerical Analysis, 2007.
[8] C. Bernardi and Y. Maday. Approximations spectrales de problemès aux limites elliptiques. Springer-Verlag, 1992.
[9] C. Bernardi and Y. Maday. Spectral methods. Handbook of numerical analysis, 5:209–485, 1997.
[10] C. Bernardi and Y. Maday. Uniform inf–sup conditions for the spectral discretization of the stokes problem. Mathematical Models and Methods in Applied Sciences, 9(03):395–414, 1999.
[11] Brezzi. On the existence, uniqueness and approximation of saddle-point problems arising from lagrangian multipliers. Revue française d'automatique, informatique, recherche opérationnelle. Analyse numérique, 8(2):129–151, 1974.
[12] E. Brown, E. Wu, W. Zipfel, and W.W. Webb. Measurement of molecular diffusion in solution by multiphoton fluorescence photobleaching recovery. Biophysical Journal, 77:2837–2849, 1999.
[13] S. Chen, J. Shen, and L.L. Wang. Generalized jacobi functions and their applications to fractional differential equations. Mathematics of Computation, 85(300), 2014.
[14] K. Diethelm and N.J. Ford. Analysis of fractional differential equations. Journal of Mathematical Analysis and Applications, 265:229–248, 2002.
[15] T. Feder, I. Brust-Mascher, J. Slattery, B. Baird, and W.W. Webb. Constrained diffusion or immobile fraction on cell surfaces: a new interpretation. Biophysical Journal, 70:2767–2773, 1996.
[16] V. Gafiychuk, B. Datsko, and V. Meleshko. Mathematical modeling of time fractional reactiondiffusion systems. Journal of Computational and Applied Mathematics, 220(1-2):215–225, 2008.
[17] R. Ghosh and W.W. Webb. Automated detection and tracking of individual and clustered cell low density lipoprotein receptor molecules. Biophysical Journal, 68:766–778, 1994.
[18] V. Girault and P.A. Raviart. Finite element methods for Navier-Stokes equations: theory and algorithms, volume 5. Springer-Verlag, 2012.
[19] R. Gorenflo and F. Mainardi. Fractional Calculus and Continuous-Time Finance III : the Diffusion Limit. Birkhäuser Basel, 2001.
[20] N.H. Katz and N. Pavlovic. A cheap Caffarelli-Kohn-Nirenberg inequality for the Navier-Stokes equation with hyper-dissipation. Geometric and Functional Analysis, 12(2):355–379, 2002.
[21] R.C. Koeller. Applcation of fractional calculus to the theory of viscoelasticity. Journal of Applied Mechanics, 51(2):229–307, 1984.
[22] D. Kusnezov, A. Bulgac, and G.D. Dang. Quantum levy processes and fractional kinetics. Physical Review Letters, 82(6):1136–1139, 1999.
[23] G. Sacchi Landriani and H. Vandeven. Polynomial approximation of divergence-free functions. Mathematics of computation, 52(185):103–130, 1989.
[24] X. Li and C. Xu. A space-time spectral method for the time fractional diffusion equation. SIAM Journal on Numerical Analysis, 47(3):2108–2131, 2009.
[25] X. Li and C. Xu. Existence and uniqueness of the weak solution of the space-time fractional diffusion equation and a spectral method approximation. Communications in Computational Physics, 8(5):1016, 2010.
[26] S. Lin and C. Xu. Theoretical and numerical investigation of fractional differential equations. Mathematica Numerica Sinica, 18(1):1–24, 2016.
[27] R.E. Lynch, J.R. Rice, and D.H. Thomas. Direct solution of partial difference equations by tensor product methods. Numerische Mathematik, 6(1):185–199, 1964.

[28] Y. Maday. Analysis of spectral projectors in one-dimensional domains. mathematics of computation, 55(192):537–562, 1990.

[29] Y. Maday, D. Meiron, A.T. Patera, and E.M. Rønquist. Analysis of iterative methods for the steady and unsteady stokes problem: Application to spectral element discretizations. SIAM Journal on Scientific Computing, 14(2):310–337, 1993.

[30] Y. Maday and A.T. Patera. Spectral element methods for the incompressible navier-stokes equations. In IN: State-of-the-art surveys on computational mechanics (A90-47176 21-64). New York, American Society of Mechanical Engineers, volume 1, pages 71–143, 1989.

[31] M.M. Meerschaert and E. Scalas. Coupled continuous time random walks in finance. Physica A Statistical Mechanics and Its Applications, 390(1):114–118, 2006.

[32] I. Podlubny. Fractional Differential Equations. Academic Press, 1999.

[33] M. Raberto, E. Scalas, and F. Mainardi. Waiting-times and returns in high-frequency finanical data: An empirical study. Physica A Statistical Mechanics and Its Applications, 314(1):749–755, 2002.

[34] S.G. Samko, A.A. Kilbas, and O.I. Marichev. Frational integrals and derivatives. Theory and Applications, Gordon and Breach, Yverdon, 1993, 1993.

[35] E. Sheets, G. Lee, R. Simson, and K. Jacobson. Transient confinement of a glycosylphosphatidylinositol-anchored protein in the plasma membrane. Biochemistry, 36:12449–12458, 1997.

[36] J. Shen, T. Tang, and L.L. Wang. Spectral methods: algorithms, analysis and applications, volume 41. Springer Science and Business Media, 2011.

[37] P. Smith, I. Morrison, K. Wilson, N. Fernandez, and R. Cherry. Anomalous diffusion of major histocompatability complex class I molecules on HeLa cells determined by single particle tracking. Biophysical Journal, 76(6):3331–3344, 1999.

[38] F. Song, C. Xu, and G.E. Karniadakis. A fractional phase-field model for two-phase flows with tunable sharpness: Algorithms and simulations. Computer Methods in Applied Mechanics and Engineering, 305:376–404, 2016.

[39] G. Szegö. Orthogonal Polynomials (fourth edition), volume 23. AMS Coll. Publ., 1975.

[40] T. Tao. Global regularity for a logarithmically supercritical hyperdissipative Navier-Stokes equation. Analysis and PDE, 2(3):361–366, 2009.

[41] W. Xiao, J. Chen, D. Fan, and X. Zhou. Global Well-Posedness and Long Time Decay of Fractional Navier-Stokes Equations in Fourier-Besov Spaces. Abstract and Applied Analysis, 2014(2):1–11, 2014.

[42] Q. Yang, F. Liu, and I. Turner. Numerical methods for fractional partial differential equations with riesz space fractional derivatives . Applied Mathematical Modelling, 34(1):200–218, 2010.

[43] X. Yu and Z. Zhai. Well-posedness for fractional Navier-Stokes equations in the largest critical spaces. Mathematical Methods in the Applied Sciences, 35(6):676C683, 2012.

[44] M. Zayernouri and G.E. Karniadakis. Fractional Sturm-Liouville eigen-problems: theory and numerical approximation. Journal of Computational Physics, 252:495–517, 2014.



School of Mathematical Sciences and Fujian Provincial Key Laboratory of Mathematical Modeling and High Performance Scientific Computing, Xiamen University, 361005 Xiamen, China.

*E-mail*: `linshimin@stu.xmu.edu.cn`

Bordeaux INP, I2M, (UMR CNRS 5295), 33607 Pessac, France.

*E-mail*: `azaiez@enscbp.fr`

Corresponding author. School of Mathematical Sciences and Fujian Provincial Key Laboratory of Mathematical Modeling and High Performance Scientific Computing, Xiamen University, 361005 Xiamen, China.

*E-mail*: `cjxu@xmu.edu.cn`